FEBS Letters 582 (2008) 1437–1443

Dynamics of Cdc42 network embodies a Turing-type mechanism of yeast cell polarity

Andrew B. Goryachev*, Alexandra V. Pokhilko

Centre for Systems Biology at Edinburgh, School of Biological Sciences, University of Edinburgh, Edinburgh EH9 3JR, United Kingdom

Received 18 March 2008; accepted 19 March 2008

Available online 31 March 2008

Edited by Felix Wieland

A.B.G. dedicates this work to his parents and D.S. Chernavskii

Abstract **Complex biochemical networks can be understood by identifying their principal regulatory motifs and mode of action. We model the early phase of budding yeast cellular polarization and show that the biochemical processes in the presumptive bud site comprise a Turing-type mechanism. The roles of the prototypical activator and substrate are played by GTPase Cdc42 in its active and inactive states, respectively. We demonstrate that the nucleotide cycling of Cdc42 converts cellular energy into a stable cluster of activated Cdc42. This energy drives a continuous membrane-cytoplasmic exchange of the cluster components to counteract diffusive spread of the cluster. This exchange explains why only one bud forms per cell cycle, because the winner-takes-all competition of candidate sites inevitably selects a single site.**

Keywords: Cell polarity; Small GTPases; Self-organization; Network motifs; Turing model; Budding yeast

1. Introduction

Emergence of cellular polarity is a symmetry-breaking event through which a cell acquires an internal structural and functional axis. This is vitally important for the cell to migrate or grow along morphogen gradients, select a direction for division, and transmit neural information [1,2]. The transition from a functionally symmetric to a polarized form is an example of pattern formation manifested by many self-organizing systems [3]. Following the pioneering work of A. Turing [4], various models of the activator–inhibitor type have been suggested to explain the spontaneous emergence of cellular polarity [5–8]. However, the specific molecular mechanisms that fit the requirements of the Turing model have been largely elusive [9] and, therefore, the applicability of the Turing theory to these systems has not been demonstrated unambiguously. Here we provide a detailed analysis of the experimentally determined molecular network that is responsible for the early phase of yeast bud formation, a prototypical example of cellular polarization [10]. We demonstrate that the molecular interactions between the small Rho GTPase Cdc42, its regulatory molecules and its effector Bem1 are sufficient to explain the spontaneous emergence of a unique yeast bud. We show that the core biochemical mechanism of this phenomenon can be described by a prototypical Turing-type model.

Importantly, we find that the polarization mechanism is fundamentally dependent on the switch-like property of small GTPases. These essential proteins normally exist in two alternative conformations: the active, when bound to a molecule of guanosine triphosphate (GTP), and the inactive, when associated with guanosine diphosphate (GDP) [1]. While in vitro small GTPases are capable of slow spontaneous nucleotide cycling [11], in vivo, their activity is tightly controlled by a number of regulatory molecules. Guanine nucleotide exchange factors (GEFs) activate the GTPases by catalyzing the replacement of bound GDP by GTP. Conversely, GTPase activating proteins (GAPs) deactivate the GTPases by facilitating the hydrolysis of GTP into GDP. In addition, GDP dissociation inhibitors (GDIs) reversibly associate with the inactive form of the Rho GTPases and participate in their membrane-cytoplasmic shuttling and intracellular transport [1].

Formation of the incipient yeast bud can be naturally subdivided into two consecutive phases [12,13]. During the short initial phase, a round cluster of activated Cdc42 forms on the inner leaflet of the plasma membrane in a location predetermined by the landmark proteins, which in haploid yeast are positioned around the bud scar remaining from the previous cell division [10]. Subsequent recruitment of the Cdc42 effectors results in the formation of actin cables and a concentric septin ring that defines the bud neck. In the ensuing phase of growth and protrusion, the actin cables serve as tracks for polarized exocytosis of vesicles that bring material for the bud growth. Importantly, it has been shown that neither actin nor landmark proteins are essential for the emergence of the Cdc42 cluster [12,14]. Instead, this phase requires the Cdc42 GEF Cdc24, the Cdc42 effector Bem1 and the ability of the GTPase to cycle between the active GTP-bound and inactive GDP-bound states [13,14]. In sharp contrast, the following actin-dependent phase has been shown to successfully proceed with a constitutively active version of Cdc42 which did not require Cdc24 or Bem1 [13,15]. In natural conditions, transport vesicles are thought to deliver inactive Cdc42 [15] whose local activation is required for polarized exocytosis at the incipient yeast bud [16]. Apart from this common requirement for Cdc42 and its regulatory molecules, the

*Corresponding author.
E-mail address: Andrew.Goryachev@ed.ac.uk (A.B. Goryachev).

Abbreviations: GEF, guanine nucleotide exchange factor; GAP, GTPase activating protein

0014-5793/$34.00
doi:10.1016/j.febslet.2008.03.029

two phases of bud formation rely on distinct molecular mechanisms. Here we focus on the formation of the Cdc42 cluster as the primary symmetry-breaking event that provides a prepattern for the subsequent morphogenesis. We assumed that the non-essential landmark proteins had been deleted [13,14] to exclude any preexisting spatial cues and that the transition to the succeeding actin-dependent phase had been arrested by treatment with latranculin A, a standard actin-depolymerizing agent. The growth and protrusion phase which is dependent on the actin-directed exocytosis has been studied in detail elsewhere [15,17] and is not considered further in this report.

2. Materials and methods

To understand emergence of the cluster of activated Cdc42 during the early phase of yeast bud formation, we developed a whole-cell model that describes reactions, membrane-cytoplasmic shuttling and diffusion of the essential molecules. It was assumed that, on the time scale of the cluster formation, production and degradation of proteins can be neglected. Therefore the total intracellular amounts of Cdc42, its GEF Cdc24 and effector Bem1 were kept constant. The resulting system of reaction–diffusion equations was simulated numerically and analyzed using several complementary methods. A detailed description of methods including the derivation of model equations, parameter selection, model analysis and its computational implementation are provided in the Supplementary Methods.

3. Results and discussion

Analysis of a large body of experimental data brought us to the conclusion that Cdc42 nucleotide cycling and membrane-cytoplasmic shuttling are the two processes responsible for the formation of the Cdc42 cluster on the membrane [13,14]. Cytoplasmic Cdc42 is the inactive GDP-bound form (RD) found in a complex with RhoGDI proteins that reversibly deposit the RD on the membrane and recycle it back to the cytoplasm [1,18] (Fig. 1E and Supplementary Methods). Cdc24 and Bem1 also shuttle between the membrane and the cytoplasm on their own or as a heterodimer. Importantly, formation of the Cdc24 · Bem1 complex increases the retention of Cdc24 on the membrane in the catalytically potent form that can activate the membrane-bound RD [14,19]. Active Cdc42 (RT) is thought to remain on the membrane until deactivated by a GAP [1] and in turn binds and activates its various effectors, including Bem1 [10,14]. The binding of Bem1 to RT recruits the Cdc24 · Bem1 complex from the cytoplasm and further increases the retention of Cdc24 through the formation of a trimolecular complex [19,20]. Once activated and stabilized on the membrane by RT and Bem1, Cdc24 in a positive feedback loop generates more membrane-bound RT at the expense of the Cdc42 cytoplasmic store [13,14,21].

3.1. Cluster of activated Cdc42 forms spontaneously in the model of bud formation

To understand the forces that drive the emergence of the Cdc42 cluster, we constructed and analyzed a detailed mathematical model of the cluster formation. Chemical reactions, membrane-cytoplasmic exchange and diffusion of all essential species were represented as a system of partial differential equations which was solved numerically (see Supplementary Methods).

In vivo, the formation of a new bud in haploid wild-type yeast is initiated by the cell-cycle regulated release of Cdc24 from the cell nucleus [22]. In silico, starting with the spatially homogeneous distribution of Cdc42 and Cdc24 · Bem1 complex in the cytoplasm and no RT on the membrane, the model evolved into a steady-state with RT uniformly distributed over the membrane. On closer investigation, this stationary state was found to be unstable to spatially heterogeneous perturbations. Astonishingly, the perturbed uniform state evolved into a striking asymmetric pattern with all RT assembled in a single round cluster with a bell-shaped concentration profile as shown in Fig. 1A. Exactly the same structure emerged when we started simulations with RT non-uniformly seeded on the membrane. Insensitive to the initial conditions, the Cdc42 cluster was found dependent on variation of the diffusion coefficients. Gradual reduction of the cytoplasmic diffusivity D_c, or increase in the membrane diffusivity D_m, resulted in spreading and eventual dissolution of the structure into a stable uniform state.

3.2. Stationary cytoplasmic flux offsets diffusive spread of the cluster

As the cluster persisted indefinitely in our simulations, we asked which mechanism counteracts the diffusion that tends to uniformly distribute RT over the membrane. We found that in the stationary state the inevitable diffusive spread of the cluster on the membrane is exactly compensated by a cytoplasmic flux of the cluster components as shown in Fig. 1. Importantly, since the active form of Cdc42 is essentially membrane-bound, the GDI-mediated membrane-cytoplasmic traffic of the GTPase is entirely determined by the balance of the cytoplasmic and membrane pools of the inactive form. Far away from the cluster, association of RD with the membrane is exactly balanced by its dissociation resulting in a steady-state membrane concentration RD_0 and a zero membrane-cytoplasmic flux $J_0 = 0$ (Fig. 1 C and D). However, in the center of the cluster, rapid activation of Cdc42 (RD → RT) by the highly concentrated GEF complex causes local depletion of RD, $RD_C < RD_0$, and thus favors the deposition of Cdc42 over its return to the cytoplasm, $J_C > 0$. As RT diffuses along the membrane away from the cluster center, the concentration of the GEF complex sharply drops and the inactivation of Cdc42 by the GAPs becomes the predominant reaction (RT → RD) (Fig. 1E). This causes local excess of RD at the cluster periphery, $RD_P > RD_0$, and, consequently, GDI-mediated dissociation of Cdc42 from the membrane, $J_P < 0$. The coupling of the Cdc42 membrane-cytoplasmic shuttling and its nucleotide cycling results in the net deposition of Cdc42 in the cluster center and the return back to the cytoplasm at the cluster periphery (Fig. 1E). GEF complex Cdc24 · Bem1 shuttles between the membrane and the cytoplasm together with Cdc42 and the steady-state profile of the Cdc24 · Bem1 flux (Fig. 1D, green) is qualitatively identical to that of Cdc42. To maintain this cyclic flux of Cdc42 in the steady-state requires a continuous supply of energy which is provided by the hydrolysis of GTP during the Cdc42 nucleotide cycling. The resulting spatial profile of the membrane-cytoplasmic transport shown in Fig. 1D is characteristic of local activation and lateral inhibition, the two fundamental properties that were found essential for the formation of spatial patterns in a variety of biological systems [3,23].

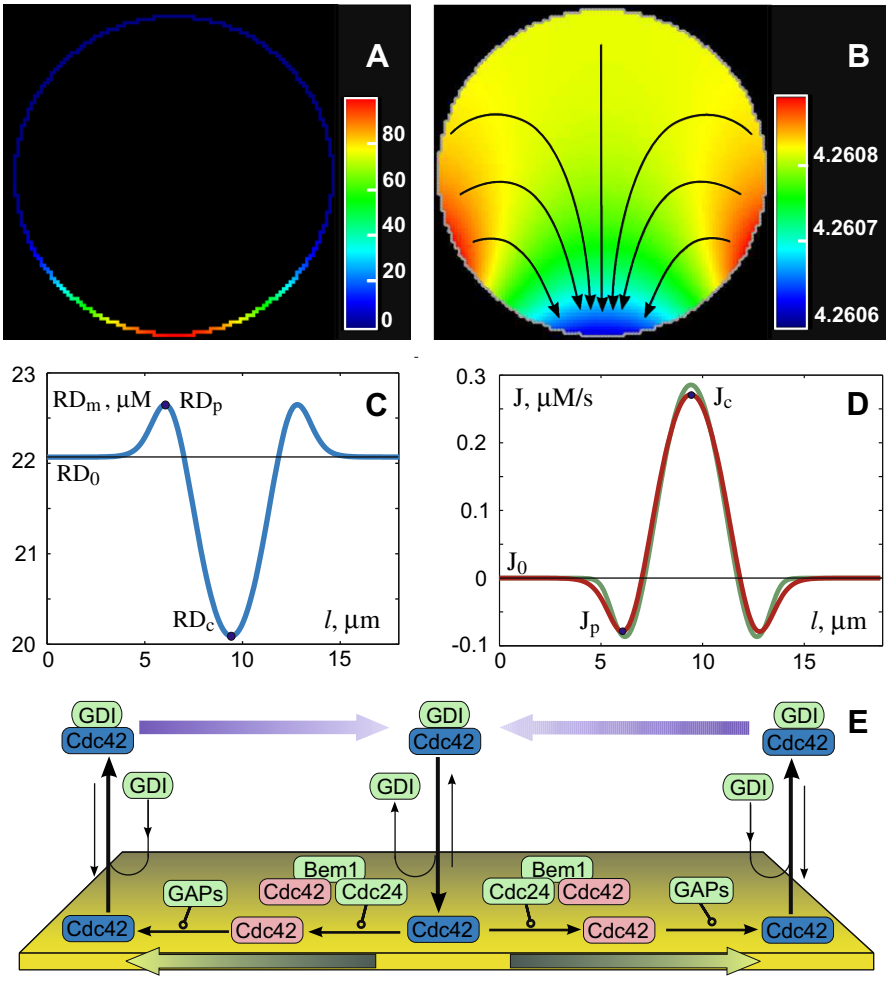

Fig. 1. Self-organized cluster of activated Cdc42 is maintained in the steady-state by a continuous membrane-cytoplasmic flux. (A and B) 2D cross-section of a yeast cell simulated with Virtual Cell [36]. (A) Distribution of the activated Cdc42 on the membrane (RT, μM) qualitatively reproduces experimental results [14,17]. (B) Concentration of the inactive Cdc42 · GDI complex in the cytoplasm (RDIc, μM). Stationary cytoplasmic flux of RDIc (arrows) compensates diffusive spread of the cluster on the membrane. (C) Steady-state profile of the inactive Cdc42 (RD) on the membrane plotted along the cellular circumference shows depletion in the cluster center and excess on its periphery. (D) Membrane-cytoplasmic fluxes of Cdc42 (red) and Cdc24 · Bem1 complex (green). Positive value indicates net flux direction towards the membrane. For visual clarity, the Cdc24 · Bem1 flux is multiplied by 10. (E) Cartoon explaining how the membrane-cytoplasmic shuttling of Cdc42 (inactive form, blue; active, pink) is coupled to its nucleotide cycling in the cluster. Thick black arrows represent the predominant direction of the membrane-cytoplasmic exchange; open circle arrowheads indicate catalysis; colored arrows represent the diffusion flux direction on the membrane and in the cytoplasm.

3.3. Cdc42 cluster is robust to parameter variation and molecular noise

Robustness to fluctuations in the reaction rates and species concentrations has been proposed as a major property of naturally evolved molecular networks. We thus set out to explore how variation of the model parameters affects the concentration profile of the Cdc42 cluster. Varying the reaction rates and computing the change in the maximum concentration and the width of the stationary RT profile, we found that the cluster is indeed largely insensitive to these variations (see Table S2 in Supplementary Methods).

More importantly, our model robustly reproduced the formation of a unique Cdc42 cluster in the experiments with deleted landmark proteins and a depolymerized actin cytoskeleton [13,14]. In the absence of spatial cues provided by the landmarks, the yeast bud is known to form at a random, yet unique, location. We simulated the emergence of the Cdc42 cluster under the conditions of molecular noise by taking into the consideration spontaneous activation of individual Cdc42 molecules on the membrane (see Supplementary Methods). This noise was sufficient to initiate the accumulation of RT on the membrane, at first without clear spatial preference (Fig. 2). However, as the accumulation continued, readily distinguishable cluster nuclei formed and competed with each other. We performed a large number of simulations varying the specific realization of the random molecular noise as well as its intensity. In all simulations, only one of the nuclei developed into a mature stationary cluster in accord with the experimental observations (see also Movie S1). This demonstrated that molecular noise is sufficient to induce spontaneous Cdc42 cluster formation. Despite random induction of multiple nucleation cores, only one mature cluster emerged from the competition of the nuclei regardless of the particular noise realization.

The standard linear stability analysis of the uniform stationary state of the model confirmed our numeric simulations and

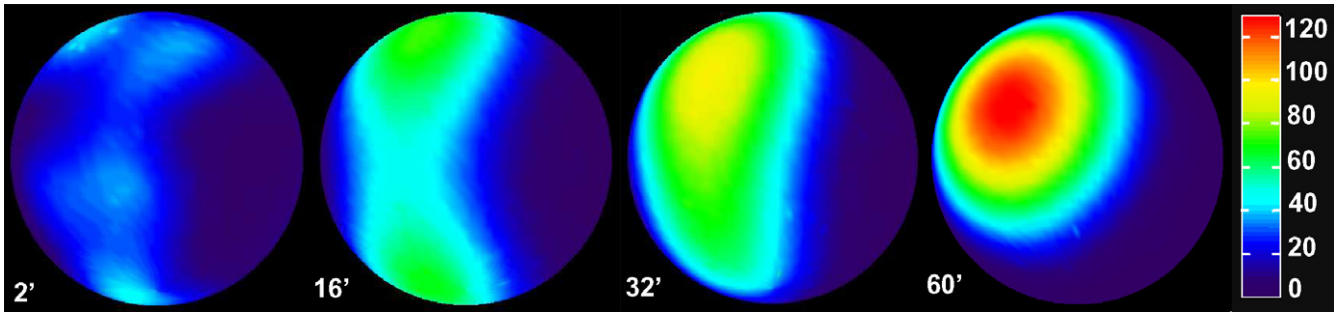

Fig. 2. A single Cdc42 cluster forms in the simulations with molecular noise. A 3D view on the surface of a yeast cell shows the distribution of the activated Cdc42 on the membrane, coded by color (RT, μM). In the absence of landmark proteins, spontaneous activation of individual Cdc42 molecules on the membrane can induce the cluster formation. Initially, all Cdc24 · Bem1 is in the cytoplasm. At first, RT accumulates at multiple random locations (2 min). Subsequently, two well-defined cluster nuclei form (16 min). The top nucleus consumes the slower-growing lower nucleus (32 min). By 1 h the Cdc42 cluster is near the steady-state.

proved that the spontaneous formation of the Cdc42 cluster observed in our in silico experiments is indeed a genuine diffusion-driven instability (Fig. S1 in Supplementary Methods). Furthermore, this analysis suggested that the structure that emerges out of the unstable uniform state could be a mixture of three distinct patterns: a single cluster, two opposing clusters and three equidistant clusters. In simulations, however, we found that patterns with multiple identical clusters are also unstable to perturbations and, once destabilized, invariably evolve into a single cluster that amasses all of the material of the initial clusters. Thus, we explain the uniqueness of the Cdc42 cluster by the competition of the candidate clusters for shared resources, the cellular stores of Cdc42, Cdc24 and especially Bem1, which is the least abundant cluster component in the yeast cell [24].

3.4. Network motif responsible for the Cdc42 cluster formation

Next, we asked which elements of the reaction network are directly responsible for the destabilization of the uniform RT distribution and the emergence of the cluster. Using the techniques of graph-theoretic analysis [25] (see Supplementary Methods), we traced the cause of the Turing-type instability in our model to the network cycle shown in Fig. 3. The cycle represents a positive feedback loop in which the membrane-bound RT recruits Cdc24 · Bem1 from the cytoplasm and forms a highly active Cdc24 · Bem1 · RT complex that generates more RT from RD [26]. In silico, we disabled the interaction between RT and the cytoplasmic Cdc24 · Bem1 (reaction v_8 in Fig. 3B). In complete agreement with the graph analysis, the disruption of this autocatalytic loop totally abrogated the formation of the Cdc42 cluster. Importantly, another autocatalytic loop, which is structurally identical to the cycle in Fig. 3 but instead involves the membrane-bound Cdc24 · Bem1 complex, cannot rescue the cluster formation (see Supplementary Methods). This striking result may be explained by the necessity to maintain the membrane-cytoplasmic circulation of the cluster components. Indeed, the interaction between the cytoplasmic Cdc24 · Bem1 and membrane-bound RT couples the spatio-temporal dynamics of Cdc24 to the GTP-driven membrane-cytoplasmic flux of Cdc42. The loss of this interaction does not prevent the autocatalytic production of RT but rather terminates the recruitment of Cdc24 from the cytoplasm into the cluster.

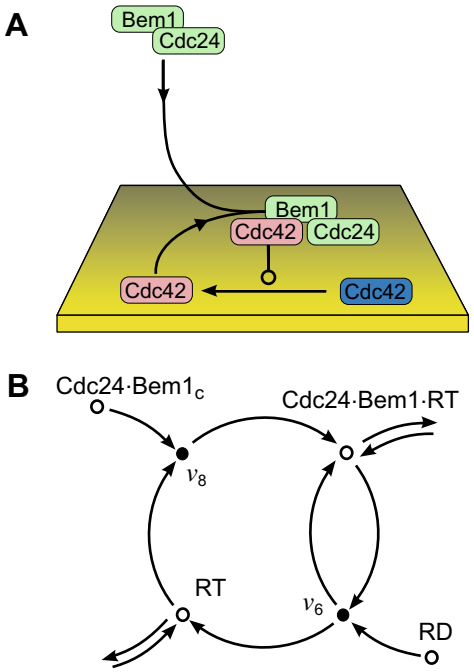

Fig. 3. Positive feedback loop with autocatalytic production of activated Cdc42 destabilizes the spatially uniform steady-state and causes the formation of the Cdc42 cluster. (A) Loop diagram, notations are the same as in Fig. 1. (B) The corresponding bi-partite reaction graph (see Supplementary Methods). Species and reactions are represented by open and filled circles, respectively. The complete reaction network graph is shown in Fig. S2.

Our results demonstrate that this process is essential for the growth and maintenance of the cluster.

3.5. Turing-type model emerges from the complete reaction–diffusion mechanism

Reduction of large models to their minimal functional form has been proven beneficial for uncovering fundamental features often buried in complex reaction mechanisms. Assuming a number of simplifying approximations (see Supplementary Methods), we reduced our complete model to a model with only two variables: RT (X) and the total concentration of the inactive Cdc42 (Y):

$$\dot{x} = E_c\alpha x^2 y + E_c\beta xy - \gamma x + D_m\Delta x,$$
$$\dot{y} = \gamma x - E_c\alpha x^2 y - E_c\beta xy + D_c\Delta y,$$
$$E_c = E_c^0\left(1 + \int_S f(x)\mathrm{d}s\right)^{-1}.$$

The last equation represents conservation of the total cellular amount of Cdc24 · Bem1. Depletion of Cdc24 · Bem1 prevents the recruitment of the entire cytoplasmic Cdc42 into the cluster and thus has to be captured by the model. The reduced model belongs to the prototypical activator–substrate type [23] in which the slowly diffusing activator X autocatalytically reproduces itself at the expense of the fast diffusing substrate Y. In our reduced model, the autocatalytic production of X occurs through the parallel cubic $2X + Y \to 3X$ and quadratic $X + Y \to 2X$ effective mechanisms that correspond to two different pathways of RT generation. The effectively cubic mechanism emerges from the reduction of the critical fragment of the complete reaction network (Fig. 3). The respective term of the reduced model, $E_c\alpha x^2 y$, essentially represents the product of three reactions: (i) recruitment of the cytoplasmic Cdc24 · Bem1 to the membrane (reaction rate proportional to the concentration of the recruiting RT, i.e., x); (ii) formation of the activated GEF complex Cdc24 · Bem1 · RT (brings in another factor x); (iii) activation of RD by the Cdc24 · Bem1 · RT complex (proportional to y). The other mechanism corresponds to the pathway that does not include the recruitment of the cytoplasmic Cdc24 · Bem1 and comprises only the reactions (ii) and (iii). The respective term, $E_c\beta xy$, is thus quadratic.

Importantly, only the cubic mechanism supports the formation of the Cdc42 cluster. The quadratic term alone was not sufficient to produce the cluster in the reduced model. This is in the complete agreement with our graph-theoretic analysis since the loss of the cubic mechanism in the reduced model is equivalent to disruption of the critical fragment shown in Fig. 3. Interestingly, cubic autocatalysis is typical for the two-variable models of pattern formation that were developed in various disciplines [27] (see Fig. 4). The apparent similarity of the reaction graphs of our model and the Brusselator highlights their common principle of pattern formation. In both models the deactivation pathway $X \to Y$ dominates at low concentrations of X. Only above a certain threshold concentration X^* does the autocatalytic production of X prevails over its deactivation and the net direction of the reaction flux reverses $Y \to X$.

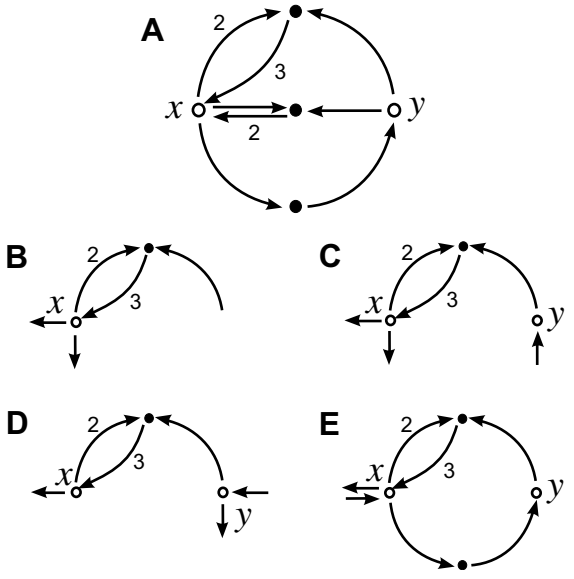

Fig. 4. The reduced model of the Cdc42 cluster formation belongs to a well-known class of activator–substrate models with autocatalysis [3]. Graph representation reveals common and divergent features of the reaction mechanisms typical of this class: (A) Reduced Cdc42 cluster formation model; (B) one-variable Schlögl model; (C) Schnakenberg model; (D) Gray-Scott model; (E) Brusselator. Species and reactions are denoted as open and filled circles, respectively. The stoichiometric coefficients on the arrows correspond to the cubic $2X + Y \to 3X$ and quadratic $X + Y \to 2X$ autocatalytic mechanisms.

4. Conclusions

Turing-type models have long been anticipated to describe the self-organized emergence of cellular polarity, however, the underlying molecular networks were largely unknown. In this study we started with the detailed, experimentally determined molecular mechanism based on the small Rho GTPase Cdc42 [26]. Using complementary methods of biophysical modeling, mathematical biology and graph-theoretic analysis we demonstrated that the molecular network consisting of Cdc42, its regulatory molecules and an effector can explain the spontaneous emergence of cellular polarization in yeast through the Turing-type instability. This phenomenon is robust to variation of reaction rates and molecular noise. Importantly, our results demonstrate that the roles of both the activator and substrate in the prototypical Turing mechanism can be played by a single molecular species with two distinct states. We hypothesize that small GTPases have evolved to perform this double function in a variety of cellular processes that require rapid formation of compact protein clusters on the membranes. This hypothesis is based on the observation that the network motif demonstrated here to be essential for the formation of the cluster is found experimentally in the rapidly increasing number of biological systems [26,28]. Indeed, GTPase effectors that recruit and activate a GEF for the same GTPase have been identified in the molecular networks that control exocytosis [29], fusion

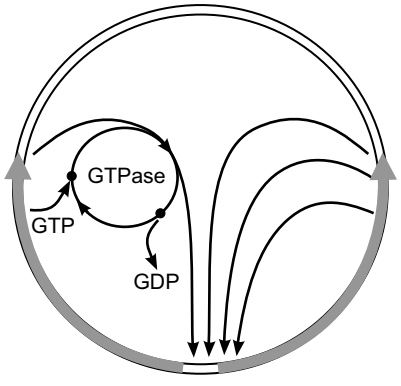

Fig. 5. Schematic representation of the mechanism underlying stable existence of the cluster of activated Cdc42 on the yeast cell membrane. Driven by the continuous expenditure of cellular energy (GTP), stationary membrane-cytoplasmic flux of cluster components (thin arrows) compensates for the inevitable diffusive spread of the cluster on the membrane (thick arrows).

of early endosomes [30] and yeast vacuoles [31]. A peculiar example of this network motif, implemented as a single protein with complex regulation, is represented by Sos (son of sevenless), the protein that possesses both the effector and GEF domains for Ras GTPase [32].

The cluster of activated Cdc42 that marks the presumptive bud site is shown here to be a true dissipative structure as defined by Ilya Prigogine [33] since its emergence and maintenance require continuous expenditure of the cellular energy stored as GTP (see Fig. 5). This explains the experimentally found requirement for the Cdc42 nucleotide cycling during which GTP is hydrolyzed. Corroborating the ideas proposed in [34], we conclude that small GTPases utilize cellular energy to combat the inevitable increase in entropy, manifested by the diffusive spread of the Cdc42 cluster on the membrane. The robust uniqueness of the yeast bud is explained in our model by the resource competition that destabilizes the coexistence of multiple buds. For a few known yeast mutants that can grow several buds simultaneously, the cause of the abnormality was traced to the altered control of nucleotide cycling [35]. It would be interesting to extend our model to incorporate these mutants and characterize the nature of multiple budding.

Acknowledgements: We thank M. Mincheva, M.R. Roussel and G. Ermakov for help with the graph-theoretic analysis of reaction networks; D.J. Lew, A.J. Millar, N.D. Read, K.E. Sawin and K.J. Painter for many stimulating discussions and helpful suggestions. A.B.G. is supported by the RCUK Academic Fellowship.

Appendix A. Supplementary data

Supplementary data associated with this article can be found, in the online version, at doi:10.1016/j.febslet.2008.03.029.

References

[1] Jaffe, A.B. and Hall, A. (2005) Rho GTPases: biochemistry and biology. Annu. Rev. Cell Dev. Biol. 21, 247–269.
[2] Fukata, M., Nakagawa, M. and Kaibuchi, K. (2003) Roles of Rho-family GTPases in cell polarisation and directional migration. Curr. Opin. Cell Biol. 15, 590–597.
[3] Maini, P.K., Painter, K.J. and Chau, H.N.P. (1997) Spatial pattern formation in chemical and biological systems. J. Chem. Soc. Faraday Trans. 93, 3601–3610.
[4] Turing, A.M. (1952) The chemical basis of morphogenesis. Philos. Trans. R. Soc. Lond. B: Biol. Sci. 237, 37–72.
[5] Meinhardt, H. (1999) Orientation of chemotactic cells and growth cones: models and mechanisms. J. Cell Sci. 112, 2867–2874.
[6] Levchenko, A. and Iglesias, P.A. (2002) Models of eukaryotic gradient sensing: application to chemotaxis of amoebae and neutrophils. Biophys. J. 82, 50–63.
[7] Narang, A. (2006) Spontaneous polarization in eukaryotic gradient sensing: a mathematical model based on mutual inhibition of frontness and backness pathways. J. Theor. Biol. 240, 538–553.
[8] Maly, I.V., Wiley, H.S. and Lauffenburger, D.A. (2004) Self-organization of polarized cell signaling via autocrine circuits: computational model analysis. Biophys. J. 86, 10–22.
[9] Maini, P.K., Baker, R.E. and Chuong, C.M. (2006) Developmental biology. The Turing model comes of molecular age. Science 314, 1397–1398.
[10] Park, H.O. and Bi, E. (2007) Central roles of small GTPases in the development of cell polarity in yeast and beyond. Microbiol. Mol. Biol. Rev. 71, 48–96.
[11] Zhang, B., Zhang, Y., Wang, Z. and Zheng, Y. (2000) The role of Mg^{2+} cofactor in the guanine nucleotide exchange and GTP hydrolysis reactions of Rho family GTP-binding proteins. J. Biol. Chem. 275, 25299–25307.
[12] Ayscough, K.R., Stryker, J., Pokala, N., Sanders, M., Crews, P. and Drubin, D.G. (1997) High rates of actin filament turnover in budding yeast and roles for actin in establishment and maintenance of cell polarity revealed using the actin inhibitor latrunculin-A. J. Cell Biol. 137, 399–416.
[13] Wedlich-Soldner, R., Wai, S.C., Schmidt, T. and Li, R. (2004) Robust cell polarity is a dynamic state established by coupling transport and GTPase signaling. J. Cell Biol. 166, 889–900.
[14] Irazoqui, J.E., Gladfelter, A.S. and Lew, D.J. (2003) Scaffold-mediated symmetry breaking by Cdc42p. Nat. Cell Biol. 5, 1062–1070.
[15] Wedlich-Soldner, R., Altschuler, S., Wu, L. and Li, R. (2003) Spontaneous cell polarization through actomyosin-based delivery of the Cdc42 GTPase. Science 299, 1231–1235.
[16] Zhang, X., Bi, E., Novick, P., Du, L., Kozminski, K.G., Lipschutz, J.H. and Guo, W. (2001) Cdc42 interacts with the exocyst and regulates polarized secretion. J. Biol. Chem. 276, 46745–46750.
[17] Marco, E., Wedlich-Soldner, R., Li, R., Altschuler, S.J. and Wu, L.F. (2007) Endocytosis optimizes the dynamic localization of membrane proteins that regulate cortical polarity. Cell 129, 411–422.
[18] Dovas, A. and Couchman, J.R. (2005) RhoGDI: multiple functions in the regulation of Rho family GTPase activities. Biochem. J. 390, 1–9.
[19] Shimada, Y., Wiget, P., Gulli, M.P., Bi, E. and Peter, M. (2004) The nucleotide exchange factor Cdc24p may be regulated by auto-inhibition. EMBO J. 23, 1051–1062.
[20] Bose, I., Irazoqui, J.E., Moskow, J.J., Bardes, E.S., Zyla, T.R. and Lew, D.J. (2001) Assembly of scaffold-mediated complexes containing Cdc42p, the exchange factor Cdc24p, and the effector Cla4p required for cell cycle-regulated phosphorylation of Cdc24p. J. Biol. Chem. 276, 7176–7186.
[21] Butty, A.C., Perrinjaquet, N., Petit, A., Jaquenoud, M., Segall, J.E., Hofmann, K., Zwahlen, C. and Peter, M. (2002) A positive feedback loop stabilizes the guanine-nucleotide exchange factor Cdc24 at sites of polarization. EMBO J. 21, 1565–1576.
[22] Gulli, M.P., Jaquenoud, M., Shimada, Y., Niederhauser, G., Wiget, P. and Peter, M. (2000) Phosphorylation of the Cdc42 exchange factor Cdc24 by the PAK-like kinase Cla4 may regulate polarized growth in yeast. Mol. Cell 6, 1155–1167.
[23] Murray, J.D. (1993) Mathematical Biology, Springer-Verlag, Berlin.
[24] Ghaemmaghami, S., Huh, W.K., Bower, K., Howson, R.W., Belle, A., Dephoure, N., O'Shea, E.K. and Weissman, J.S. (2003) Global analysis of protein expression in yeast. Nature 425, 737–741.
[25] Mincheva, M. and Roussel, M.R. (2006) A graph-theoretic method for detecting potential Turing bifurcations. J. Chem. Phys. 125, 204102.
[26] Goryachev, A.B. and Pokhilko, A.V. (2006) Computational model explains high activity and rapid cycling of Rho GTPases within protein complexes. PLoS Comput. Biol. 2, e172.
[27] Tyson, J.J. and Light, J.C. (1973) Properties of two-component bimolecular and trimolecular chemical reaction systems. J. Chem. Phys. 59, 4164–4172.
[28] Grosshans, B.L., Ortiz, D. and Novick, P. (2006) Rabs and their effectors: achieving specificity in membrane traffic. Proc. Natl. Acad. Sci. USA 103, 11821–11827.
[29] Medkova, M., France, Y.E., Coleman, J. and Novick, P. (2006) The rab exchange factor Sec2p reversibly associates with the exocyst. Mol. Biol. Cell 17, 2757–2769.
[30] Lippe, R., Miaczynska, M., Rybin, V., Runge, A. and Zerial, M. (2001) Functional synergy between Rab5 effector Rabaptin-5 and exchange factor Rabex-5 when physically associated in a complex. Mol. Biol. Cell 12, 2219–2228.
[31] Wurmser, A.E., Sato, T.K. and Emr, S.D. (2000) New component of the vacuolar class C-Vps complex couples nucleotide exchange on the Ypt7 GTPase to SNARE-dependent docking and fusion. J. Cell Biol. 151, 551–562.
[32] Margarit, S.M., Sondermann, H., Hall, B.E., Nagar, B., Hoelz, A., Pirruccello, M., Bar-Sagi, D. and Kuriyan, J. (2003) Structural

evidence for feedback activation by Ras · GTP of the Ras-specific nucleotide exchange factor SOS. Cell 112, 685–695.
[33] Glansdorff, P. and Prigogine, I. (1971) Thermodynamic Theory of Structure, Stability and Fluctuations, John Wiley, New York.
[34] Goody, R.S. (2003) The significance of the free energy of hydrolysis of GTP for signal-transducing and regulatory GTPases. Biophys. Chem. 100, 535–544.
[35] Caviston, J.P., Tcheperegine, S.E. and Bi, E. (2002) Singularity in budding: a role for the evolutionarily conserved small GTPase Cdc42p. Proc. Natl. Acad. Sci. USA 99, 12185–12190.
[36] Schaff, J., Fink, C.C., Slepchenko, B., Carson, J.H. and Loew, L.M. (1997) A general computational framework for modeling cellular structure and function. Biophys. J. 73, 1135–1146.